Environmental Science & Technology

Article

pubs.acs.org/est

Assessing and Forecasting Atmospheric Outflow of α-HCH from China on Intra-, Inter-, and Decadal Time Scales

Chongguo Tian,[†,‡,*] Jianmin Ma,[§] Yingjun Chen,[†] Liyan Liu,[‡] Wanli Ma,[‡] and Yi-Fan Li[‡,§]

[†]Key Laboratory of Coastal Zone Environmental Processes, Yantai Institute of Coastal Zone Research (YIC), Chinese Academy of Sciences (CAS); Shandong Provincial Key Laboratory of Coastal Zone Environmental Processes, YICCAS, Yantai Shandong 264003, P. R. China

[‡]International Joint Research Center for Persistent Toxic Substances (IJRC-PTS), State Key Laboratory of Urban Water Resource and Environment, Harbin Institute of Technology, Harbin 150090, P. R. China

[§]Air Quality Research Division, Science and Technology Branch, Environment Canada, 4905 Dufferin Street, Toronto, Ont, M3H 5T4, Canada

Supporting Information

ABSTRACT: Atmospheric outflow of α-HCH from China from 1952 to 2009 was investigated using Chinese Gridded Pesticide Emission and Residue Model (ChnGPERM). The model results show that the outflows via the northeast boundary (NEB, longitude 115−135 °E along 55 °N and latitude 37−55 °N along 135 °E) and the mid-south boundary (MSB, longitude 100−120 °E along 17 °N) of China account for 47% and 35% of the total outflow, respectively. Two climate indices based on the statistical association between the time series of modeled α-HCH outflow and atmospheric sea-level pressure were developed to predict the outflow on different time scales. The first index explains 70/83% and 10/46% of the intra-annual variability of the outflow via the NEB and MSB during the periods of 1952−1984 and 1985−2009, respectively. The second index explains 16% and 19% of the interannual and longer time scale variability in the outflow through the NEB during June−August and via the MSB during October−December for 1991−2009, respectively. Results also revealed that climate warming may potentially result in stronger outflow via the NEB than the MSB. The linkage between the outflow with large scale atmospheric circulation patterns and climate warming trend over China was also discussed.

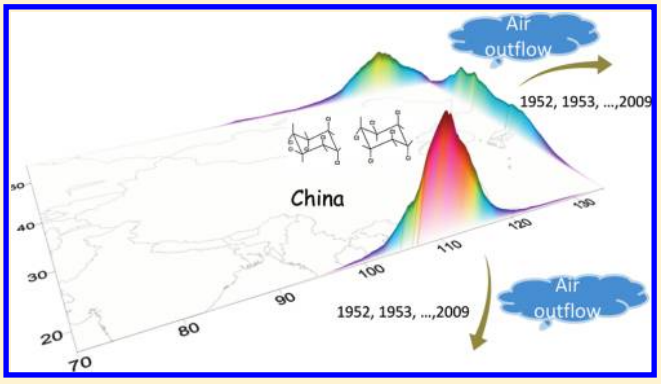

INTRODUCTION

Rapid population and economic growth in China have led to a rapid increase in emission of anthropogenic air pollutants. The atmospheric outflows of these pollutants and their contamination to downstream environments have now become an international concern.[1] There is abundant evidence of carbon monoxide (CO), polycyclic aromatic hydrocarbons (PAHs), and other air pollutants exporting from Asia/China.[2−6] This has inspired a number of studies for the association of atmospheric outflow of air pollutants from Asia/China with climate. For example, the interannual variation of CO outflow to west Pacific has been demonstrated to be influenced by the frequency of cold surges in spring.[7] Liang et al. developed meteorological indices to explain the variances in the eastward CO outflow from Asia.[8] Lang et al. found that the interannual variation of the eastward outflow of PAHs from China is positively correlated with cold episodes of El Niño-Southern Oscillation.[9]

Differing from CO and PAHs which are still extensively emitted into the atmosphere by their respective primary emission sources, following the worldwide bans and restrictions, regional cycling and global distribution of persistent organic pollutants (POPs) have become governed primarily by secondary emissions from terrestrial surfaces contaminated previously. Reemission of POPs from these secondary emission sources is strongly affected by temperature.[10,11] This has been shown by lower air concentration of those banned POPs during the wintertime,[12] due largely to low air temperatures which lock POPs in surface media. It is expected that, although wind regimes over China during the wintertime favors long-range atmospheric transport (LRAT) of legacy POPs,[2,3,7] such transport and outflow are less significant for this cold season because the relatively lower air concentration is more readily dispersed in the atmosphere. However, little attention has been paid to the combined impact of wind system and temperature on the atmospheric outflow of legacy POPs from Asia/China.

Received: August 16, 2011
Revised: December 31, 2011
Accepted: January 18, 2012
Published: January 18, 2012

α-hexachlorocyclohexane (HCH), listed recently as a new POP by Stockholm Convention,[13] is the most representative isomer of technical HCH. China was the largest user of technical HCH in the world.[14] To date, the use of α-HCH in China has been banned for more than two decades.[15] This enables us to investigate its outflow during the periods of its application and when the secondary reemission dominates. Because Eastern China has been identified as a major source of α-HCH globally,[14] and its external sources only exert a weak influence on the α-HCH budget in Chinese environment,[16] Chinese sources of α-HCH were only considered here. The present study aims at identifying and predicting the variability in α-HCH atmospheric outflow on various time scales and its association with climate through extensive model simulations from 1952, when China began to use the pesticide, to 2009 using a multimedia mass-balance model. The objectives are (1) to identify and assess the outflow characteristic and major outflow boundaries in China; (2) to develop meteorological indices used to predict intra-, interannual and longer time scale variability of the outflow; and (3) to assess the potential influence of climate warming on the changes in the α-HCH outflow from China.

MATERIALS AND METHODS

Modeling. α-HCH outflow from China was simulated by Chinese Gridded Pesticide Emission and Residue Model (ChnGPERM). The ChnGPERM was developed based on Gridded Basin-based Pesticide Mass Balance Model (GB-PMBM). The model has been applied in a previous modeling study for α-HCH budget in Taihu region, China.[17] Briefly, it is a gridded mass balance model with 1/6° latitude by 1/4° longitude resolution spanning 17−55 °N and 70−135°E, as shown in Figure S1 of the Supporting Information (SI). Four matrixes, air, water, soil, and sediment, are included in the model. There are five soil types in the model, including dry cropland, paddy field, forestry, grassland, and uncultured land. In the soil matrixes, the model adopts four well-mixed soil layers, with depths at 0.1, 1.0, 20, and 30 cm from top to bottom. There are two vertical layers in the model atmosphere. The first layer is the atmospheric boundary layer (ABL) with a depth of 1000 m and the second layer is the atmospheric low troposphere (ALT) extending from 1000 to 4000 m height. The model includes transfer and transport modules. The transfer module describes the changes in concentrations and inter-compartmental transfer/exchange of the substance among the multimedia environments, including soil, water, sediment, and the air compartment in the ABL. The transport module solves horizontal and vertical mass exchange of the chemical between different grid cells in the ABL and ALT. The detailed structure and physical/chemical processes included in the model were referred to Tian et al.[16,17]

The numerical simulation was performed successively from 1952 to 2009 at the time step of 1 day. The input data include physicochemical properties of α-HCH (see Table S1 of the SI),[16] gridded usage inventory of α-HCH, and gridded environmental data. By assuming 67.5% composition of α-HCH in technical HCH,[18] gridded annual usage of α-HCH from 1952 to 1984 (see Figure S1 of the SI) was derived from a gridded technical HCH usage inventory in China.[15] The model environmental and geophysical data include daily meteorological data, soil characteristic, and land use over the model domain. The meteorological (winds, temperature, precipitation) data from 1952 to 2009 at the ChnGPERM model grids of 1/6° × 1/4° latitude/longitude were interpolated, using the Canadian Meteorological Centre's objective analysis and interpolation system, from the daily objectively analyzed data with spatial spacing of 2.5° × 2.5° latitude/longitude from the United States National Center for Environmental Prediction (NCEP) reanalysis.[19] The gridded soil characteristic data were also interpolated from a global soil data with 1° latitude by 1° longitude resolution.[20] The land use data were compiled by using an advanced high-resolution radiometer global land data.[15]

Seasonal atmospheric concentrations of α-HCH in 37 Chinese cities from a field campaign in 2005[12] were used for model evaluation. Further insight into the model performance was also gained from the comparison between modeled air concentrations and available fragmentary measurements of α-HCH air concentrations across China spanning 1979 to 2009, collected from literatures. Results show that the model captures to a large extent the temporal and spatial variations of α-HCH concentration in the atmosphere across China (Figures S2−4, Table S2, and text in the SI).

The model uncertainty was evaluated by Monte Carlo simulation. In the uncertainty analysis, the model was run 1000 times to calculate α-HCH concentrations with randomly generated input parameters with their respective coefficient of variation based on the probability distributions. For each run, the calculated concentrations over the model domain were averaged and the result showed a typical normal distribution, as shown by Figure S5 in the SI which presents a typical case for the model uncertainty analysis using the model output air concentrations in 1980. Details of the uncertainty analysis are presented in Table S3, Figures S2 and S5, and text in the SI.

Meteorological Indices. Two meteorological indices were developed, based on statistical relationships between α-HCH outflow and atmospheric sea level pressure (SLP), to predict the α-HCH outflow from China on intra-, inter-annual and longer time scale. To quantify the α-HCH atmospheric outflow from China, the α-HCH-laden air mass reaching the model lateral boundaries was defined as the α-HCH outflow mass. The atmospheric outflow of α-HCH was computed as the total outflow mass of α-HCH in both ABL and ALT. The SLP is a major meteorological variable connecting with background atmospheric circulation and climate that drive atmospheric transport of air pollutants from daily to interannual time scales.[8,21−23] The SLP data were also collected from the NCEP reanalysis with a 2.5° × 2.5° resolution.[19]

The associations between the α-HCH outflow and SLP were determined by the Pearson correlation. The time series of standardized α-HCH outflow and SLP anomalies by their respective standard deviations were used for the statistical analysis. The SLP in a certain region of the model domain with strong positive and/or negative correlation was adopted to develop the meteorological indices. As will be elaborated in next section, the first meteorological index predicting the intra-annual variation of the α-HCH outflow from China was derived by regressing the time series of monthly α-HCH outflow anomalies, standardized by the annual standard deviation of the substance, to the gridded SLP anomalies, also standardized by its annual standard deviation. This regression analysis was performed for two time periods. The first period spans 1952 to 1984 during which α-HCH was still in use. In this period, the regression analysis may help to distinguish the outflow features induced by atmospheric circulation patterns, the application, and reemission of the chemical. The second period covers

1985−2009 after the primary emission of α-HCH was terminated in China, in order to highlight the influence of atmospheric circulation and reemission on the α-HCH outflow.

Since the primary emission of α-HCH before its ban often dominates its spatial and temporal distribution, it is not straightforward to identify the interannual and longer time scale variations of the α-HCH outflow driven by atmospheric circulations. Therefore, to develop the second meteorological index which addresses the interannual and longer time scale change in the α-HCH outflow from China, the present study examined the variation of the α-HCH outflows from 1991 to 2009 during which the use of the pesticide has completely ceased (or the illegal use becomes minimum), as well as the linkage of the outflow with the interannual and longer time scale change in the SLP.

A detrending method was used in the annual time series of α-HCH atmospheric outflows. This technique has been used to extract climate signals from the temporal trend of POPs in the atmosphere measured over the Great Lakes[24] and the Arctic.[11] Following these studies, we removed the both linear trend of the time series of standardized α-HCH outflow anomalies and the first autocorrelation from the α-HCH time series, in order to unveil potential climate signals from a "noise" background of the modeled time series of α-HCH outflow. A fugacity method developed by Harner et al.[25] was used to calculate the response of α-HCH reemission from soil to air temperatures.

RESULTS AND DISCUSSION

Modeling Atmospheric Outflow of α-HCH. A fifty-eight year model simulation shows that the total outflow mass of α-HCH from 1952 to 2009 is 79.5 kilotons, in which 99.5% occurred during 1952−1984, the period when the pesticide was in use in China.[15] The percentage of α-HCH outflow through the four model lateral boundaries in the two model atmospheric layers from 1952 to 2009 is summarized and displayed in Figure 1. In the ABL, the atmospheric concentration outflow accounts for 53% of the total outflow, and the rest occurs in the ALT depending on the strength of westerly wind in this layer, agreeing with the Asian CO outflow pattern reported by Bey et al.[2] The outflows through the west boundary can be ignored because α-HCH-laden air masses from Eastern China sources seldom approach the west boundary (e.g., Tibetan plateau) under prevailing westerly wind over midlatitudes.[2,7,8] Two major outflow pathways can be identified from Figure 1, one across the northeast corner of the model domain, termed in the present study as the Northeast Boundary (NEB, crossing longitude 115−135 °E along 55°N and latitude 37−55°N along 135 °E), and the other passing through the south boundary, termed as the Mid-south Boundary (MSB, crossing longitude 100−120 °E along 17 °N). The modeled outflows through the NEB and MSB account for 47% and 35% of the total outflow from 1952 to 2009, respectively.

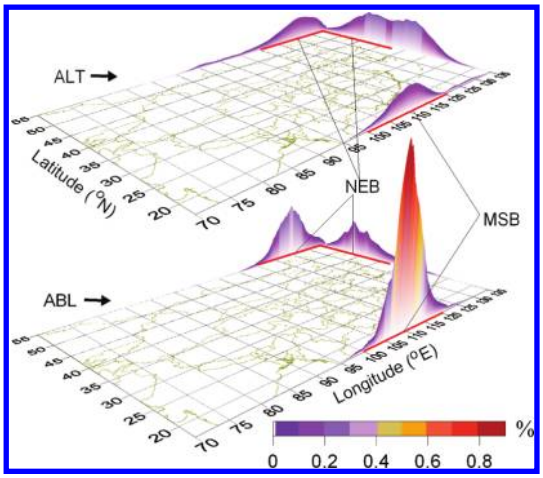

Figure 1. Percentage of atmospheric outflows of α-HCH (contoured) via ABL and ALT from four boundaries of model domain from 1952 to 2009. The red solid lines indicate the major outflow pathways termed as NEB and MSB, respectively.

Figure S6 of the SI illustrates annual net atmospheric transport fluxes of α-HCH in both atmospheric layers in 1960, 1980, 2000, and 2009 respectively, calculated as the sum of the monthly averaged daily α-HCH air concentration fluxes ($=V \times C_a$, where V is horizontal wind components and C_a is air concentration). The annual net transport fluxes reveal a significant atmospheric transport route from south to north in Eastern China within the ABL, especially before 1984 when the pesticide was heavily used in Southeastern China.[15] This suggests that the major outflow of α-HCH takes place in the northeast boundary of the model domain, rather than the southeast boundary. Another appreciable atmospheric route for α-HCH outflow can be identified in the southern boundary of the model domain. In the ALT (free atmosphere), however, the α-HCH laden air exhibits an eastward transport pattern. This is driven by prevailing westerly winds over midlatitudes.[2,7,8] Iwata et al. also reported that α-HCH concentrations in the atmosphere and seawater near the NEB and MSB, collected from five cruises field investigations during 1989−1990, were higher compared with α-HCH levels near other model boundaries.[26]

Figure S7 of the SI displays monthly percentage of α-HCH outflow mass via the NEB and MSB for 1952−1984 and 1985−2009, respectively. The outflow through the NEB mainly occurred in summer (June−August) whereas the outflow via the MSB mostly took place in the period of autumn−winter (October−December). The summer outflow pattern via the NEB appears associated with Eastern Asian summer monsoon, characterized by strong southerly and southeasterly winds extending from Southeastern to Northeastern China.[27] This wind regime provided a vehicle for northward atmospheric transport of α-HCH laden air from Southeastern China, where the pesticide was used largely,[15] to Northeastern China. A previous study has identified significant α-HCH outflows in the summertime[28] and found that Northeastern China was a prominent sink region of α-HCH emitted from Southeastern China sources, driven by the summer monsoon circulation and other environmental factors.[16] Harner et al. reported higher α-HCH concentrations in the mid-troposphere over the west coast of Canada, collected from an aircraft measurement in August 2001, and inferred the higher concentrations to α-HCH emission from Northeastern China.[29] It has been also reported that the maximum export of CO from Asia/China to the western Pacific occurred between 30 and 60 °N during summer associated with Asian summer monsoon.[8] On the other hand, it was reported that the outflow of air pollutants from Southern China mostly took place in September[30] and winter.[31] The difference in the outflow between 1952−1984 and 1985−2009 could be largely ascribed to the intermittent use of the pesticide during 1952−1984. Stronger outflow via the MSB in September and October during 1952−1984 has been found to be associated with the application of the pesticide for

dx.doi.org/10.1021/es202851n | Environ. Sci. Technol. 2012, 46, 2220−2227

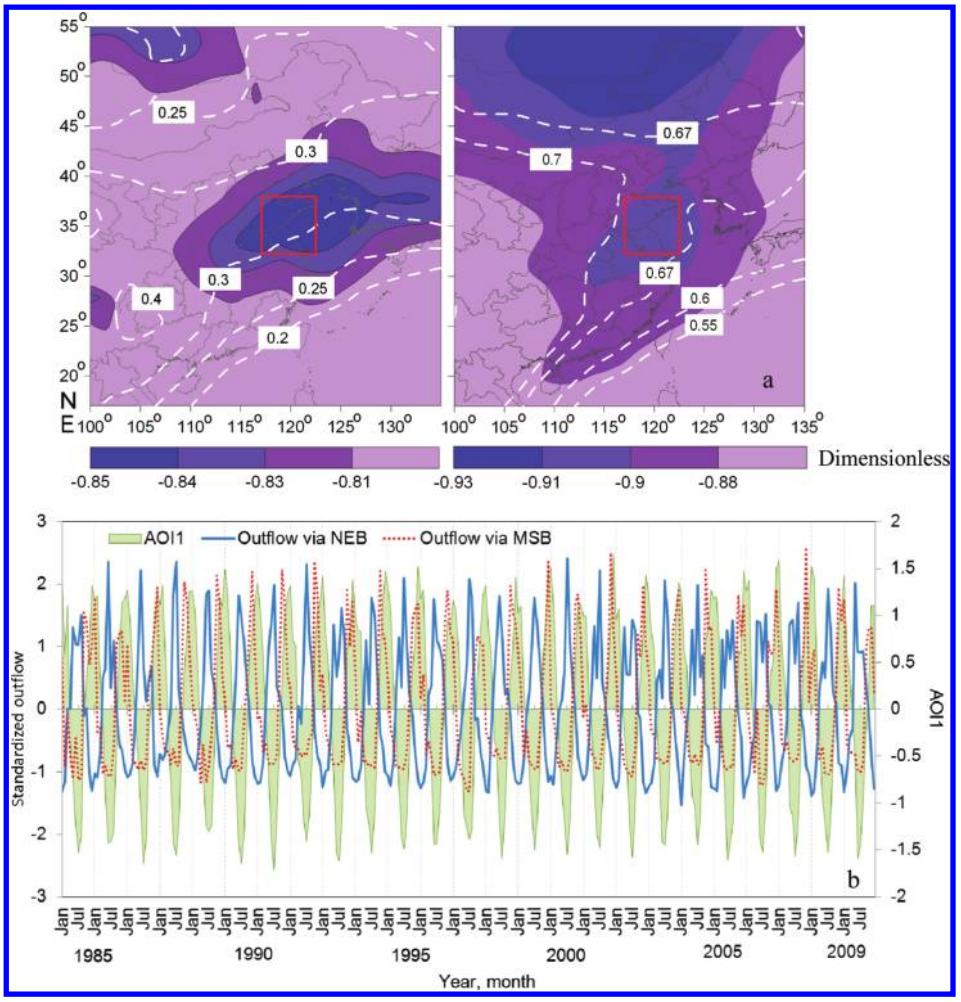

Figure 2. (a) Correlation map between monthly time series of standardized α-HCH outflow anomalies via NEB (color-contoured), MSB (white dashed lines), and SLP anomaly during 1952−1984 (left panel) and 1985−2009 (right panel). The red box is the region used defining AOI1. The correlation is significant at greater than or equal to the 90% confidence level for $r > 0.2$. (b) Monthly time series of standardized α-HCH outflow anomalies via NEB and MSB, and AOI1 during 1985−2009.

preventing winter-wheat midge occurring in autumn in China.[32] These results suggest that the variation in atmospheric outflow of banned POPs, largely dominated by environmental factors, is considerably different from those contaminants driven by direct (primary) air emission, for example, CO^{2-4} and PAHs.[9] Hence, legacy POPs outflow from China need to be properly assessed, in order to provide a new knowledge in understanding the significance of the outflow of those POPs from China in their global budget.

Meteorological Index for Intra-Annual α-HCH Outflow. Although the NEB and MSB account for only 19% and 8% of the total boundary of the model domain, α-HCH outflows through the NEB and MSB account for 47% and 35% of the total outflow from China, respectively, with obvious seasonal variation. The overwhelming α-HCH outflows through the NEB and MSB of China may provide a considerable insight into the interaction between the atmospheric circulation/climate activities and air contaminant out of China at NEB/MSB on different time scales. Understanding these atmospheric circulation patterns that drive α-HCH outflows through the NEB and MSB of China may further help us to forecast toxic outflows from China and their contribution to the global budget.

Figure 2a provides a correlation map between α-HCH outflows via the NEB and the MSB, and the SLP. In general, the SLP correlates negatively with the outflow through the NEB and positively with the outflow via the MSB. The positive and negative correlation coefficients for the second period (1985−2009), after the use of the pesticide ceased, are greater than that derived from the first period (1952−1984). Strong correlations (either positive or negative) for the two periods occur in the region spanning 117−123° E and 32−38° N, located near the eastern seaboard of China (red box in Figure 2a). These correlations suggest that the α-HCH outflow through the NEB is associated with anomalous low atmospheric pressure in Eastern China and the outflow through the MSB is correlated with anomalous high pressure in Eastern China.

Based on the above spatial correlation analysis we can then define a meteorological index to describe and monitor the background climate/atmospheric circulation pattern that drives the intra-annual atmospheric outflow of α-HCH from China. This index is termed as the atmospheric outflow index 1 (AOI1), computed by standardized monthly SLP anomalies averaged over the region where there exist large values of

dx.doi.org/10.1021/es202851n | Environ. Sci. Technol. 2012, 46, 2220−2227

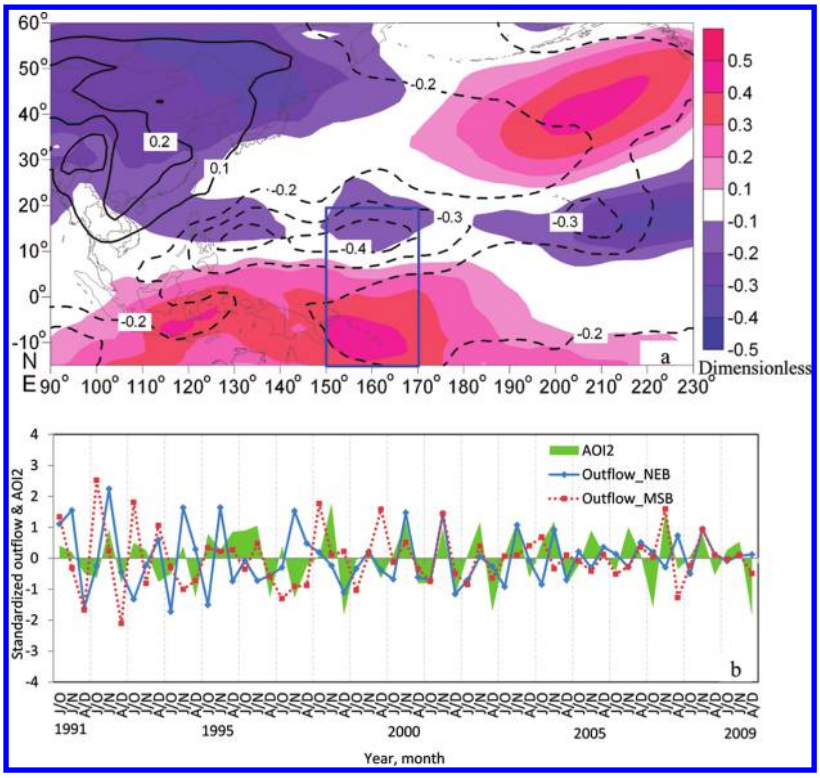

Figure 3. (a) Correlation map between monthly time series of detrended standardized α-HCH outflow anomalies via NEB for June-August (color-contoured), MSB for October- December (black lines), and SLP anomaly during 1991−2009. The blue box is the region used defining AOI2. The correlation is significant at greater than or equal to the 90% confidence level for $r > 0.3$. (b) Monthly time series of detrended standardized α-HCH outflow anomalies via NEB (solid blue line) for June-August, MSB (dashed red line) for October−December, and AOI2 (shaded green) during 1991−2009. J/O, J/N, and A/D at x-axis stand for June/October, July/November, and August/December, respectively. The symbols before and after the solidus are for the outflow via NEB and MSB, respectively.

statistical significant positive and negative correlation coefficients (117−123° E and 32−38° N, red box in Figure 2a),

$$\mathrm{AOI1} = \frac{\frac{1}{n}\sum_{i=1}^{n}\Delta P_i}{\sigma} \quad (1)$$

where n (n = 9) is the number of grid cells in the region, and ΔP_i represents the standardized SLP anomalies at a model grid i of the region, and σ is the standard deviation of the area-averaged SLP (numerator).

Monthly time series of the standardized α-HCH outflow through the NEB and MSB, and the AOI1 during 1952−1984 and 1985−2009 are plotted in Figure S8 of the SI and Figure 2b, respectively. The index can explain 70% (r = −0.84, p < 0.001, n = 396) and 10% (r = 0.31, p < 0.001, n = 396) variance of α-HCH outflow through the NEB and MSB during the first period of 1952−1984, respectively. For the second period (1985−2009), the index AOI1 explains 83% variance of the outflow (r=-0.91, p < 0.001, n = 300) from the NEB and 46% (r = 0.68, p < 0.001, n = 300) from the MSB. The statistical significance indicates that the index is a useful tool to predict the intra-annual α-HCH outflow, especially after 1984 when the primary emission ceased and the secondary emission sources started to dominate the α-HCH emissions. Predominant outflows via the NEB occurred in summer (June−August) when the lower SLP, a reflection of the summer monsoon low pressure system,[27] dominated Eastern China. Major outflows via the MSB occurred during the transition period from autumn to winter (October−December) but the higher SLP mainly occurred during the wintertime (December and February of the following year), as shown in Figure 2b (red dashed lines). To examine the influence of temperature on α-HCH outflow capacity, we estimated the response of α-HCH reemission from soil to air temperatures (see the Materials and Methods section).[25] Result shows that reemission intensity of α-HCH at 25 °C is 20% greater than that at 20 °C (see Figure S9 of the SI). Averaged temperature difference between autumn and winter in Southern China ranges from 5 to 10 °C.[12] The model calculation shows that the reemission intensity in winter reduces at least 20% from its value in autumn. In general, the index yields poorer prediction of the monthly outflow of α-HCH via the MSB than that from the NEB.

Meteorological Index for Interannual and Longer Time Scale α-HCH Outflow. As aforementioned, the strongest α-HCH outflows were found from June to August via the NEB and from October to December through the MSB. The outflows of α-HCH during these two periods via the NEB and MSB account for 46% and 65% of their total outflow during 1991−2009, respectively. Therefore, to elucidate possible relationships between the variation in the α-HCH outflow and the SLP, we shall focus on the monthly outflows via the NEB during June−August and via the MSB during October−December for 1991−2009. Figure S10 of the SI illustrates standardized monthly α-HCH outflows via the NEB (June to August) and MSB (October to December) during 1991−2009. As seen from the figure, both time series exhibit a statistical significant downward trend during this period. To unveil their temporal variability on both interannual and decadal scale, we first detrend the time series of the

dx.doi.org/10.1021/es202851n | Environ. Sci. Technol. 2012, 46, 2220−2227

standardized monthly α-HCH outflow anomalies and then regress the detrended time series into the corresponding monthly SLP anomaly time series from 1991 to 2009, also standardized by its standard deviations. Results are shown in Figure 3a. As seen, there are large positive correlation coefficients centered at 10°S, 160°E ($r > 0.4$) for the summer α-HCH outflow via the NEB, and large negative correlations centered at 10°N, 160°E ($r < -0.4$) for the autumn−winter α-HCH outflow via the MSB, respectively.

Based on these correlation analyses, we can now develop the second atmospheric outflow index, AOI2. The AOI2 is calculated using the weighted SLP anomalies averaged over the area extending from 15°S to 20° N, and from 150° to 170° E, highlighted by the blue box in Figure 3a,

$$\mathrm{AOI2} = \frac{\frac{1}{n}\sum_{i=1}^{n}[(r_i \times \Delta P_i)_{\mathrm{NEB}} + (r_i \times \Delta P_i)_{\mathrm{MSB}}]}{\sigma} \quad (2)$$

where n ($n = 135$) is the number of model grid cells within the highlighted region, r is the correlation coefficient between standardized SLP anomalies, ΔP, in the region and standardized α-HCH outflow anomalies, and σ is the standard deviation of the term in the numerator of eq 2.

Figure 3b displays the AOI2 and the detrended outflow time series for 1991−2009 via the NEB and MSB. The AOI2 explains 16% ($r = 0.40$, $p < 0.01$, $n = 57$) and 19% ($r = 0.44$, $p < 0.005$, $n = 57$) variance of the interannual and longer time scale atmospheric outflow of α-HCH through the NEB during June−August and via the MSB during October−December, respectively.

Interestingly, the highlighted region (blue box, Figure 3a), where there exist strong correlation coefficients between α-HCH outflow and the SLP time series, coincides with well-known Indo-Pacific warm water pool (IPWWP, see Figure S11 of the SI). It has been well documented that ocean-atmosphere interactions in the tropical Pacific region strongly affect global atmospheric circulation,[33] global heat and water vapor transport.[34] Changes in sea surface temperature (SST) and the atmospheric convection in the IPWWP are largely responsible for the interannual to decadal climate variability in extra-tropical regions.[33−35] The IPWWP can extend to Southern China Sea, considerably influencing the wind and atmospheric pressure patterns in South China.[36] As shown in Figure 3a, the positive correlation indicates that the interannual and longer time scale α-HCH outflow in the summertime via the NEB is associated with abnormally higher SLP over the IPWWP. This suggests a stronger northward atmospheric pressure gradient and hence a stronger southerly summer monsoon wind regime, favoring northward atmospheric transport and outflow of α-HCH through the NEB. On the other hand, the negative correlation between the α-HCH outflow via the MSB and the SLP time series in the period of autumn-winter indicates that stronger outflows via the MSB are associated with abnormally lower SLP over the IPWWP. This suggests a stronger southward atmospheric pressure gradient from Southern China to the Southern China Sea, causing a stronger northerly wind regime over this region. This atmospheric pressure and wind regime favor southward atmospheric transport. These wind regimes were demonstrated by the analyses of wind anomalies over Eastern China in winter[36] and in summer[37] associated with the SST over the IPWWP.

Potential Influence of Climate Change on α-HCH Outflow. Since the results presented above have linked the α-HCH outflow from China with air temperature, it is worthwhile to extend the investigation to the potential impact of climate change on the outflow. Because higher air temperatures may result in stronger reemission of POPs to the air from those sinks where POPs were locked and accumulated from their past application and deposition, increasing efforts have been devoted to the study for the POPs revolatilization and recirculation from their repositories incurred by climate warming.[11,24] Like most places in the world, China also experienced climate warming over the last half century.[38] Figure S12 of the SI illustrates the trend of annual mean surface air temperature (SAT) over the model domain from 1991 to 2009. Over China, stronger warming trend occurred in Southeastern China, the region coinciding with the major source region of α-HCH in China.[15] However, the time series of the α-HCH outflow shows a decreasing trend (Figure S10 of the SI) during this period, which is opposite of expected increasing trend of the outflow associated with the increasing α-HCH reemission under a warming climate. This declining trend was largely due to the decrease of α-HCH environmental residues in China because of its removal and environmental degradation process.[16,28] As a result, the declining trend overwhelmed the underlying signals of climate warming[11] in the modeled α-HCH outflow time series. Considering that the reemission of α-HCH from its reservoirs responds more strongly to the change in air temperature, we used the detrended annual time series of standardized α-HCH outflow anomalies to detect potential signals of the warming atmosphere in the annual time series of α-HCH atmospheric outflows. Figure 4 shows the annual time series of standardized α-HCH outflow anomalies via the NEB and MSB and their respective detrended time series from 1991 through 2009. The annual averaged SAT anomalies, standardized by its standard deviation averaged over Southeastern China (blue box in Figure S12 of the SI) are also plotted here. Negative correlation between α-HCH outflow anomalies via the NEB ($r = -0.68$, $p < 0.001$), MSB ($r = -0.74$, $p < 0.001$), and the standardized SAT anomalies suggests that the decrease of total residues of α-HCH, largely due to its environmental degradation,[16] dominates the change in the α-HCH outflow. After the overwhelming declining trends were removed, the detrended α-HCH outflow via the NEB shows increasing

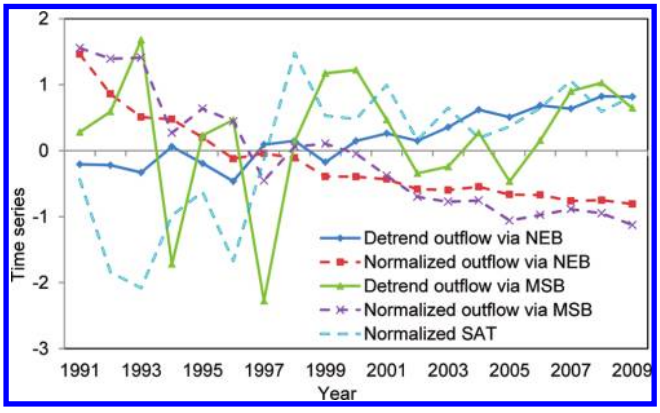

Figure 4. Detrended and standardized time series of annual α-HCH outflow anomalies via NEB and MSB from 1991 through 2009. Standardized surface air temperature (SAT) anomaly (shallow blue dish line) over Southeastern China is also presented.

trends, corresponding well to increasing mean SAT (r = 0.68, p < 0.001, n = 19). However, this good relationship does not apply for the correlation between the detrended α-HCH outflow through the MSB and the SAT (r = 0.03, p = 0.9, n = 19). This implies that stronger warming condition in China in the summers of 1991−2009 influenced more strongly on summer α-HCH outflow via the NEB, as compared to that in autumn−winter over China with weaker warming condition, especially over Southeastern China. This can be illustrated by the trend of seasonal SAT over the model domain during June−August, and October−December from 1991 to 2009 (Figure S13 of the SI). As shown, there is a stronger warming trend during June−August than that during October−December, corresponding to the more significant increase of the detrended α-HCH outflow via the NEB in the summertime. This confirms that climate warming plays an important role in environmental fate and outflow of POPs.[11]

In summary, this study developed two meteorological indices to forecast α-HCH outflow from China based on statistical significant relationships between the fluctuation of α-HCH outflow and atmospheric circulation patterns on different temporal scales which exert an strong influence on climate over China. Results presented here demonstrated that these two climate indices thoroughly explains the intra-annual, inter-annual and longer time scale variability in α-HCH outflow from China. The two indices can be extended to predict and assess the outflow pattern of those toxic substances having similar physicochemical properties as α-HCH characterized by the secondary emission from China. For those banned and restricted POPs, it is expected that climate change will play an increasing important role in their long-term trend and mobilization in environments, as addressed by recent United Nations Environment Programme (UNEP)/Arctic Monitoring and Assessment Programme (AMAP) report[39] on climate impact on POPs, and the Task Force on Hemispheric Transport of Air Pollution (HTAP) 2010 assessment report.[40] Results presented here will help to improve our understanding to the potential impacts of climate change and variability on LRAT of POPs and provide further support to recent international efforts in this aspect.

■ ASSOCIATED CONTENT

Supporting Information

Detailed information on model domain, input data, model evaluation, uncertainty analysis, annual net transport flux, monthly atmospheric outflow, time series of α-HCH outflow and AOI1 during 1952−1984, air emission from soil at different temperature, SST characterizing the Indo-Pacific warm pool, linear trend of annual and seasonal mean SAT over China. This material is available free of charge via the Internet at http://pubs.acs.org.

■ AUTHOR INFORMATION

Corresponding Author

*Phone: (86) 535-2109-160; fax: (86) 535-2109-000; e-mail: cgtian@yic.ac.cn.

■ ACKNOWLEDGMENTS

This work was supported by the Knowledge Innovation Program of the Chinese Academy of Sciences (No. KZCX2-YW-GJ02), Open Project of State Key Laboratory of Urban Water Resource and Environment, Harbin Institute of Technology (No. HC201019), and the Natural Scientific Foundation of China (Nos. 41101495 and 40806048). We gratefully acknowledge Global Soil Data Task and National Centers for Environmental Prediction for providing the Environmental data.

■ REFERENCES

(1) Pochanart, P.; Wild, O.; Akimoto, H., Air pollution import to and export from East Asia. In *The Handbook of Environmental Chemistry*; Stohl, A., Ed.; Springer-Verlag: Heidelberg, 2004; Vol. 4, pp 99−130.

(2) Bey, I.; Jacob, D.; Logan, J.; Yantosca, R. Asian chemical outflow to the Pacific in spring: Origins, pathways, and budgets. *J. Geophys. Res.* **2001**, *106* (D19), 23097−23113, DOI: 10.1029/2001JD000806.

(3) Liang, Q.; Jaeglé, L.; Jaffe, D. A.; Weiss-Penzias, P.; Heckman, A.; Snow, J. A. Long-range transport of Asian pollution to the northeast Pacific: Seasonal variations and transport pathways of carbon monoxide. *J. Geophys. Res.* **2004**, *109* (D23), D23S07 DOI: 10.1029/2003jd004402.

(4) Jaffe, D.; Anderson, T.; Covert, D.; Kotchenruther, R.; Trost, B.; Danielson, J.; Simpson, W.; Berntsen, T.; Karlsdottir, S.; Blake, D. Transport of Asian air pollution to North America. *Geophys. Res. Lett.* **1999**, *26* (6), 711−714.

(5) Zhang, Y.; Shen, H.; Tao, S.; Ma, J. Modeling the atmospheric transport and outflow of polycyclic aromatic hydrocarbons emitted from China. *Atmos. Environ.* **2011**, *45* (17), 2820−2827.

(6) Zhang, Y.; Tao, S.; Ma, J.; Simonich, S. Transpacific transport of benzo[a]pyrene emitted from Asia. *Atmos. Chem. Phys.* **2011**, *11* (23), 11993−12006.

(7) Liu, H.; Jacob, D.; Bey, I.; Yantosca, R.; Duncan, B.; Sachse, G. Transport pathways for Asian pollution outflow over the Pacific: Interannual and seasonal variations. *J. Geophys. Res.* **2003**, *108* (D20), 8786 DOI: 10.1029/2002JD003102.

(8) Liang, Q.; Jaeglé, L.; Wallace, J. M. Meteorological indices for Asian outflow and transpacific transport on daily to interannual timescales. *J. Geophys. Res.* **2005**, *110* (D18), D18308 DOI: 10.1029/2005JD005788.

(9) Lang, C.; Tao, S.; Liu, W.; Zhang, Y.; Simonich, S. Atmospheric transport and outflow of polycyclic aromatic hydrocarbons from China. *Environ. Sci. Technol.* **2008**, *42* (14), 5196−5201.

(10) Wania, F.; Haugen, J.; Lei, Y.; Mackay, D. Temperature dependence of atmospheric concentrations of semivolatile organic compounds. *Environ. Sci. Technol.* **1998**, *32* (8), 1013−1021.

(11) Ma, J.; Hung, H.; Tian, C.; Kallenborn, R. Revolatilization of persistent organic pollutants in the Arctic induced by climate change. *Nat. Clim. Change* **2011**, *1* (5), 255−260.

(12) Liu, X.; Zhang, G.; Li, J.; Yu, L.; Xu, Y.; Li, X.; Kobara, Y.; Jones, K. C. Seasonal patterns and current sources of DDTs, chlordanes, hexachlorobenzene, and endosulfan in the atmosphere of 37 Chinese cities. *Environ. Sci. Technol.* **2009**, *43* (5), 1316−1321.

(13) Vijgen, J.; Abhilash, P.; Li, Y. F.; Lal, R.; Forter, M.; Torres, J.; Singh, N.; Yunus, M.; Tian, C.; Schäffer, A.; Weber, R. Hexachlorocyclohexane (HCH) as new Stockholm Convention POPs-a global perspective on the management of Lindane and its waste isomers. *Environ. Sci. Pollut. Res.* **2011**, *18* (2), 152−162.

(14) Li, Y.; Macdonald, R. Sources and pathways of selected organochlorine pesticides to the Arctic and the effect of pathway divergence on HCH trends in biota: A review. *Sci. Total Environ.* **2005**, *342* (1−3), 87−106.

(15) Li, Y.; Cai, D.; Shan, Z.; Zhu, Z. Gridded usage inventories of technical hexachlorocyclohexane and lindane for China with 1/6° latitude by 1/4° longitude resolution. *Arch. Environ. Contam. Toxicol.* **2001**, *41* (3), 261−266.

(16) Tian, C.; Liu, L.; Ma, J.; Tang, J.; Li, Y. Modeling redistribution of α-HCH in Chinese soil induced by environment factors. *Environ. Pollut.* **2011**, *159* (10), 2961−2967.

(17) Tian, C.; Li, Y.; Jia, H.; Wu, H.; Ma, J. Modelling historical budget of α-hexachlorocyclohexane in Taihu Lake, China. *Chemosphere* **2009**, *77* (4), 459−464.

(18) Li, Y.; Cai, D.; Singh, A. Technical hexachlorocyclohexane use trends in China and their impact on environment. *Arch. Environ. Contam. Toxicol.* **1998**, *35* (4), 688−697.
(19) Kalnay, E.; Kanamitsu, M.; Kistler, R.; Collins, W.; Deaven, D.; Gandin, L.; Iredell, M.; Saha, S.; White, G.; Woollen, J.; Zhu, Y.; Leetmaa, A.; Reynolds, B.; Chellia, M.; Ebisuzaki, W.; Higgins, W.; Janowiak, J.; Mo, K.; Ropelewski, C.; Wang, J.; Jenne, R.; Joseph, D. The NCEP/NCAR reanalysis project. *Bull. Am. Meteorol. Soc.* **1996**, *77*, 437−471.
(20) Global Soil Data Task. Global gridded surfaces of selected soil characteristics (IGBPDIS). International geosphere-biosphere programme—Data and information services. Oak Ridge National Laboratory, Oak Ridge, Tennessee, U.S.A. http://www.daac.ornl.gov/ (accessed July, 1, 2002).
(21) Smith, T. M.; Arkin, P. A.; Sapiano, M. R. P. Reconstruction of near-global annual precipitation using correlations with sea surface temperature and sea level pressure. *J. Geophys. Res.* **2009**, *114* (D12), D12107 DOI: 10.1029/2008jd011580.
(22) Stammer, D.; Hüttemann, S. Response of regional sea level to atmospheric pressure loading in a climate change scenario. *J. Clim.* **2008**, *21* (10), 2093−2101.
(23) Hui, G. Comparison of East Asian winter monsoon indices. *Adv. Geosci.* **2007**, *10*, 31−37.
(24) Gao, H.; Ma, J.; Cao, Z.; Dove, A.; Zhang, L. Trend and climate signals in seasonal air concentration of organochlorine pesticides over the Great Lakes. *J. Geophys. Res.* **2010**, *115* (D15), D15307 DOI: 10.1029/2009JD013627.
(25) Harner, T.; Bidleman, T. F.; Jantunen, L. M. M.; Mackay, D. Soil-air exchange model of persistent pesticides in the United States Cotton Belt. *Environ. Toxicol. Chem.* **2001**, *20* (7), 1612−1621.
(26) Iwata, H.; Tanabe, S.; Sakel, N.; Tatsukawa, R. Distribution of persistent organochlrines in the oceanic air and surface seawater and the role of ocean on their global transport and fate. *Environ. Sci. Technol.* **1993**, *27* (6), 1080−1098.
(27) Ding, Y.; Chan, J. The East Asian summer monsoon: An overview. *Meteorol. Atmos. Phys.* **2005**, *89* (1−4), 117−142.
(28) Tian, C.; Ma, J.; Liu, L.; Jia, H.; Xu, D.; Li, Y. A modeling assessment of association between East Asian summer monsoon and fate/outflow of α-HCH in Northeast Asia. *Atmos. Environ.* **2009**, *43* (25), 3891−3901.
(29) Harner, T.; Shoeib, M.; Kozma, M.; Gobas, F. A. P. C; Li, S. M. Hexachlorocyclohexanes and endosulfans in urban, rural, and high altitude air samples in the Fraser Valley, British Columbia: Evidence for trans-pacific transport. *Environ. Sci. Technol.* **2005**, *39* (3), 724−731.
(30) Zhang, G.; Li, J.; Cheng, H.; Li, X.; Xu, W.; Jones, K. C. Distribution of organochlorine pesticides in the northern South China Sea: Implications for land outflow and air-sea exchange. *Environ. Sci. Technol.* **2007**, *41* (11), 3884−3890.
(31) Lang, C.; Tao, S.; Zhang, G.; Fu, J.; Simonich, S. Outflow of polycyclic aromatic hydrocarbons from Guangdong, Southern China. *Environ. Sci. Technol.* **2007**, *41* (24), 8370−8375.
(32) Hu, J.; Zhu, T.; Li, Q., Organochlorine pesticides in China. In *Persistent Organic Pollutants in Asia: Sources, Distributions, Transport and Fate*; Li, A., Tanabe, S., Jiang, G., Giesy, J. P., Lam, P. K. S., Eds.; Elsevier Ltd: Oxford, 2007; Vol. *7*, pp 159−211.
(33) Oppo, D. W.; Rosenthal, Y.; Linsley, B. K. 2,000-year-long temperature and hydrology reconstructions from the Indo-Pacific warm pool. *Nature* **2009**, *460* (7259), 1113−1116.
(34) Cane, M. A. A role for the tropical Pacific. *Science* **1998**, *282* (5386), 59−61.
(35) Hoerling, M. P.; Hurrell, J. W.; Xu, T. Tropical origins for recent North Atlantic climate change. *Science* **2001**, *292* (5514), 90−92.
(36) Liu, Q.; Jiang, X.; Xie, S. P.; Liu, W. T. A gap in the Indo-Pacific warm pool over the South China Sea in boreal winter: Seasonal development and interannual variability. *J. Geophys. Res.* **2004**, *109* (C07), C07012 DOI: 10.1029/2003JC002179.
(37) Xie, S. P.; Chang, C. H.; Xie, Q.; Wang, D. Intraseasonal variability in the summer South China Sea: Wind jet, cold filament, and recirculations. *J. Geophys. Res* **2007**, *112*, C10008 DOI: 10.1029/2007JC004238..
(38) IPCC. *Climate Change 2007: Synthesis Report*, Fourth Assessment Report; Intergovernmental Panel on Climate Change: Geneva, 2007; p 104, http://www.ipcc.ch/.
(39) UNEP/AMAP. *Climate Change and POPs: Predicting the Impacts. Report of the United Nations Environment Programme/Arctic Monitoring and Assessment Programme Expert Group*; Secretariat of the Stockholm Convention: Geneva, 2011; p 62, http://chm.pops.int/Implementation/GlobalMonitoringPlan/.
(40) HTAP. *Hemispheric Transport of Air Pollution 2010. Part C: Persistent Organic Pollutants*; The United Nations Economic Commission for Europe: New York and Geneva, 2011; p 236, http://www.htap.org/.